Nanoscale

Accepted Manuscript

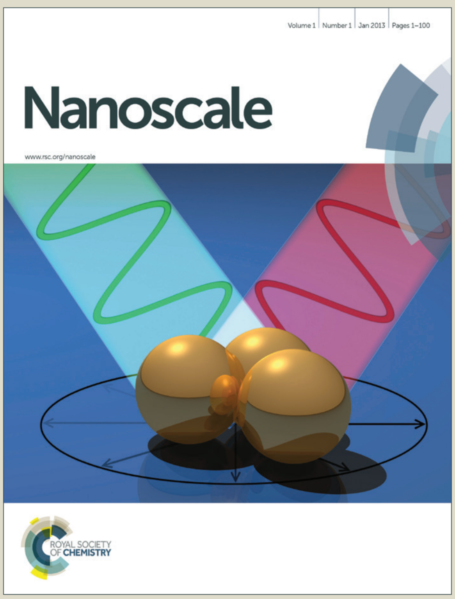

Nanoscale RSCPublishing

PAPER

Defect-Free Zinc-Blende Structured InAs Nanowires Realized by in-situ Two-V/III-Ratio Growth in Molecular Beam Epitaxy

Cite this: DOI: 10.1039/x0xx00000x

Zhi Zhang,[a] Zhen-Yu Lu,[b] Ping-Ping Chen,[b] Wei Lu,[b] and Jin Zou*[a,c]

Received 00th January 2012,
Accepted 00th January 2012

DOI: 10.1039/x0xx00000x

www.rsc.org/

In this study, we devised a two-V/III-ratio procedure to control the Au-assisted growth of defect-free InAs nanowires in molecular beam epitaxy. The demonstrated two-V/III-ratio procedure consists of a first high-V/III-ratio growth step to prepare the nanowire foundation on the substrate surface, followed by a low-V/III-ratio step to induce the nanowire growth. By manipulating the V/III ratios in different steps, we have achieved the controlled growth of pure defect-free zinc-blende structured InAs nanowires on the GaAs $\{\bar{1}\bar{1}\bar{1}\}$ substrates. This study provides an approach to control not only the crystal structure of semiconductor nanowires, but also their structural qualities.

Introduction

One-dimensional III-V compound semiconductor nanowires have attracted extensive research interest in recent years due to their distinct physical properties and hence potential applications in nanoelectronics and optoelectronics.[1-4] Currently, the most adopted techniques to grow epitaxial III-V nanowires are metal-organic chemical vapor deposition (MOCVD),[5-7] molecular beam epitaxy (MBE)[8-10] and chemical beam epitaxy[11] through the vapor-liquid-solid mechanism[12] or vapor-solid-solid mechanism.[13]

In order to achieve the practical applications of nanowires in nanodevices, it is of critical importance to control their crystal structure and structural quality. It has been found that most epitaxial III-V nanowires are generally grown along the $<000\bar{1}>$ for the wurtzite structured nanowires or along the $<\bar{1}\bar{1}\bar{1}>$ directions for zinc-blende structured nanowires.[14-18] However, the majority of epitaxial $<000\bar{1}>/<\bar{1}\bar{1}\bar{1}>$ III-V nanowires naturally contain planar defects due to the small energetic differences of the stacking sequences in wurtzite and zinc-blende structures along their $<000\bar{1}>/<\bar{1}\bar{1}\bar{1}>$ directions. In this regard, several approaches have been employed to control the structural quality of III-V nanowires, such as, varying the nominal V/III ratio in MOCVD,[19-22] adopting a two-temperature process,[23, 24] introducing a small amount of dopant to nanowires,[25] and using different kinds of catalyst (such as Pd).[26] Recently, the growth of III-V nanowires in the non-$<000\bar{1}>/<\bar{1}\bar{1}\bar{1}>$ growth directions has been reported, and these nanowires are generally defect-free and adopt zinc-blende structure.[27-31] It has been well documented that Au-catalyzed III-V nanowires grown by MBE prefer to adopt the wurtzite structure with planar defects,[32-34] and only very few studies have reported the growth of zinc-blende structured InAs nanowires in MBE.[30, 31] Based on our previous study on the investigations of InAs nanowires grown under a given V/III ratio at various V/III ratios on the GaAs $\{\bar{1}\bar{1}\bar{1}\}$ substrates in MBE,[35] we found that the nanowire growth windows of varying the V/III ratio is narrow. With a relatively high V/III ratio, conventional vertical nanowires with defected wurtzite structure can be obtained. With reducing the V/III ratio, inclined nanowires with defect-free zinc-blende structure can be obtained with a tendency of the lower the V/III ratio, the more the defect-free inclined nanowires as long as the V/III ratio is within the growth window. Since both conventional vertical nanowires and inclined nanowires are always co-existed, alternative strategies should be developed to secure the growth of defect-free zinc-blende structured nanowires exclusively on the GaAs $\{\bar{1}\bar{1}\bar{1}\}$ substrates.

In this study, we demonstrate a two-step growth to induce pure defect-free zinc-blende structured InAs nanowires on the GaAs $\{\bar{1}\bar{1}\bar{1}\}$ substrates, in which two V/III ratios were used during the InAs nanowire growth. In the first step, a high V/III ratio is used to prepare the nanowire foundation on the substrate surface; which is followed by the second step where the nanowire growth is taken place at a low V/III ratio to induce high-quality zinc-blende structured nanowires.

Experimental

The InAs nanowires were grown on the GaAs $\{\bar{1}\bar{1}\bar{1}\}$ substrates in a Riber 32 MBE system using coated Au as catalysts and with In as the indium source and As_4 as the arsenic source. The substrate surface was first degassed in the MBE preparation chamber at 250

°C, then was transferred to the growth chamber to be thermally deoxidized at 610 °C. After that, for each growth, a thin GaAs buffer layer was grown on the GaAs $\{\bar{1}\bar{1}\bar{1}\}$ substrate at 580 °C to achieve atomically flat surface. The substrate was then transferred back to the preparation chamber, and a thin Au film was deposited on the top of the GaAs buffer layer by vacuum thermal evaporation. The Au-coated GaAs substrate was finally transferred to the growth chamber, and annealed at 500 °C for 5 min under arsenic ambient to agglomerate the Au thin film into nanoparticles. After the annealing, the substrate temperature was lowered to 400 °C and the indium source was introduced to initiate the InAs nanowire growth at different V/III ratios. To achieve the growth of exclusively defect-free zinc-blende structured nanowires on the GaAs $\{\bar{1}\bar{1}\bar{1}\}$ substrates, a two-step growth was employed with the first step using a high-V/III ratio followed by a low-V/III-ratio in the second step.

The morphological characteristics of the as-grown InAs nanowires and their bases were investigated by scanning electron microscopy (SEM, JEOL 7800F, operated at 10 kV), and their detailed structural characteristics were investigated by transmission electron microscopy (TEM, Philips Tecnai F20, operated at 200 kV). Individual nanowires for TEM analysis were prepared by ultrasonicating the as-grown nanowire samples in ethanol and then dispersing individual nanowires onto holey carbon films, supported by the Cu grids.

Results and discussion

Fig. 1a and 1b show a top-view and a side-view SEM images taken from a nanowire sample grown under a V/III ratio of ~45 first for 30 min followed by a V/III ratio of ~15 for 15 min (the switch of V/III ratio was conducted in-situ to avoid the interruption of the growth). From which two kinds of nanowires can be seen: (1) long nanowires with vertical bottom section and kinked top section and (2) short inclined nanowires with irregular morphology. To clarify the growth behaviors of these nanowires, we repeated the InAs nanowire growth with the growth terminated after the first step (i.e. InAs nanowires were grown under a single high V/III ratio of ~45). Fig. 1c is a titled SEM image taken from this sample, in which two features associated with catalysts can be seen: in addition to those Au catalysts induced vertical nanowires, many Au catalysts failed to induce the nanowire growth, and they stationarily stayed on the substrate surface. Interestingly, such Au catalysts are always located on the tops of triangular pyramids (arrowed in Fig. 1c), which is formed by the attraction of indium through surface diffusion during the growth.[32] This result suggests that in our two-V/III-ratio grown nanowires, for the long nanowires, the vertical sections correspond to the first step, while the kinked sections are related to the second step. On the other hand, the short nanowires were grown only in the second step and originated from those triangular pyramids on the substrate surface.

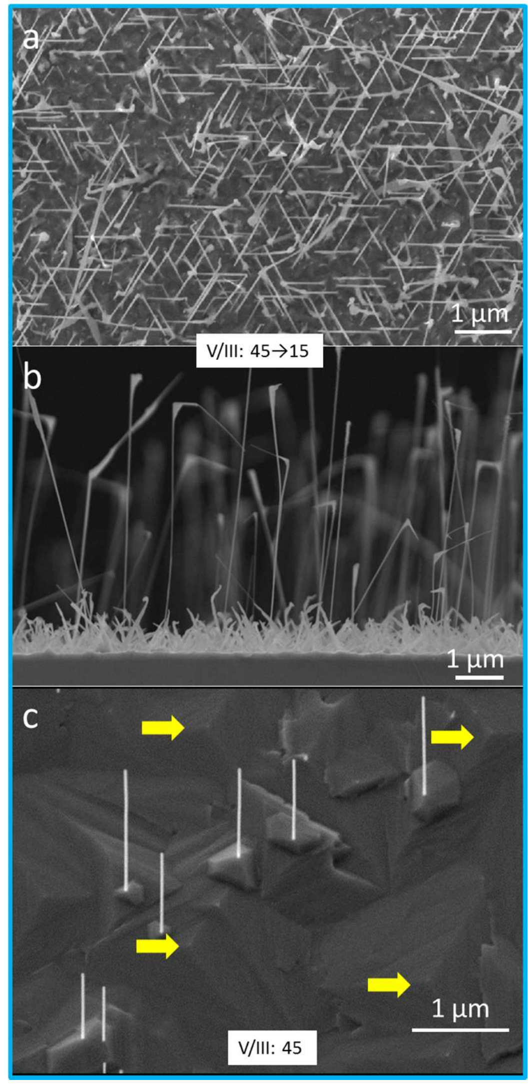

Fig. 1(a) Top-view SEM image and (b) side-view SEM image of InAs nanowires grown by a two-V/III-ratio procedure. (c) Tilt SEM image of InAs nanowires grown by a single-V/III-ratio at ~45.

To understand the structural characteristics of these long and short nanowires, TEM investigations were performed on over a dozen of nanowires from each type. Fig. 2a shows a bright-field TEM image of a typical long nanowire, from which the kinked morphology can be clearly observed. The inset is a <11$\bar{2}$0> zone-axis high-resolution TEM (HRTEM) image showing that the vertical section adopts the wurtzite structure with many planar defects. Our extensive HRTEM studies confirmed the nature of defected wurtzite structure in the vertical section of the long nanowires. On the other hand, Fig. 2b shows the overview of a typical short inclined nanowire, in which the nanowire shows irregular morphology, which is consistent with our SEM study (as can be seen from Fig. 1b, the morphology of inclined nanowires is not well controlled and the inclined features tend to be random). Fig. 2c is a bright-field TEM image taken from the middle of the nanowire, from which many planar defects can be clearly observed. Fig. 2d is the corresponding <110> zone-axis HRTEM image of the nanowire, and shows that the short nanowire has the zinc-blende structure with planar defects on their {111} atomic planes, which is different to the long nanowires with the wurtzite structure. By investigating over a dozen of short nanowires, this defected zinc-blende structure characteristic can be confirmed. It is of interest to note that, the imperfection of the side-walls of these short inclined nanowires are caused by locations of planar defects, leading to irregular side-walls (arrowed in Fig. 2c).

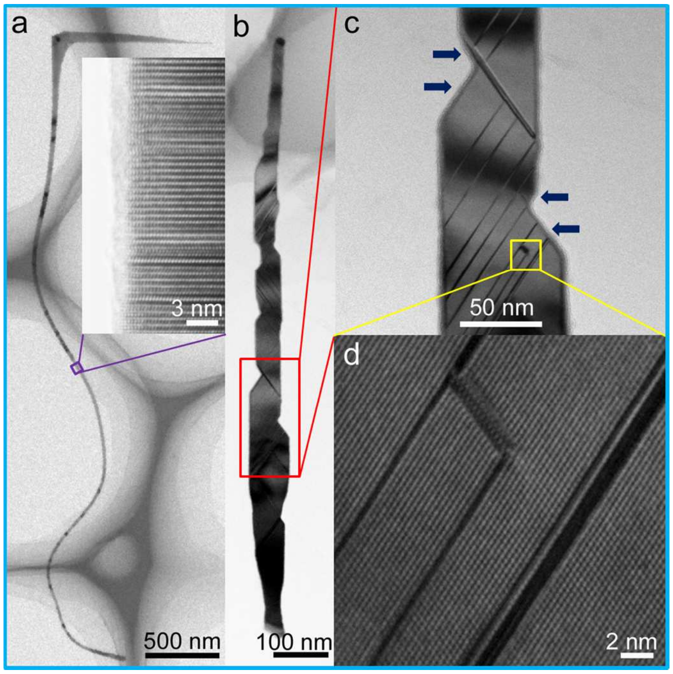

Fig. 2 TEM investigations of both kinds of InAs nanowires. (a) The overview of a typical long nanowire with inset of HRTEM image showing defected wurtzite structure. (b) The overview of a typical short inclined nanowire. (c) Bright-field TEM image taken from a section of the nanowire shown in (b). (d) HRTEM image taken from the marked area in (c).

Based on the experimental results outlined above, we anticipate that using the two-V/III-ratio procedure may induce the growth of pure defect-free zinc-blende structured InAs nanowires. Based on Fig. 1c, the growth with a high V/III ratio of ~45 leads to the formation of both vertical nanowires and triangular pyramids with Au catalysts on their tops. Since these vertical nanowires have the defected wurtzite structure (refer to Fig. 2a), they need to be restrained. Therefore, during the first step of the two-V/III-ratio procedure, the V/III ratio should be further increased to secure the formation of triangular pyramids only on the substrate surface. To clarify this assumption, we performed a nanowire growth with a single-V/III-ratio ratio ~55, and Fig. 3a shows the result where a tilt SEM image shows only triangular pyramids are formed.

On the other hand, the quality of short inclined nanowires in our two-V/III-ratio grown nanowires is poor (refer to Fig. 2b), which may be due to the V/III ratio in the second step being set too low.[35] In this regard, in order to improve the structural quality of these short nanowires, a relatively higher V/III ratio should be set in the second step. Accordingly, we redesign a two-V/III-ratio procedure to exclusively grow defect-free zinc-blende structured InAs nanowires on the GaAs $\{\bar{1}\bar{1}\bar{1}\}$ substrates. In this case, we set the growth to initiate at a high V/III ratio of ~55 for 35 min, then switch to a low V/III ratio of ~20 for 7 min. Fig. 3b is the top-view SEM image taken from this newly designed sample, and shows many inclined nanowires with certain orientations grown on the substrate. Based on the fact the cleavage planes of zinc-blende structured GaAs are {110} planes, the crystallographic orientation of the substrate can be determined, as marked in Fig. 3b. Therefore, the projections of the inclined nanowires with respect to the GaAs $\{\bar{1}\bar{1}\bar{1}\}$ substrate surface can be determined as the <112> directions, suggesting that the growth directions of these inclined nanowires are <*mmn*> where *m* and *n* are integers if the nanowires adopt the zinc-blende structure. Fig. 3c is a side-view SEM image, in which only inclined nanowires were found to be grown directly from the substrate as expected, and these inclined nanowires tend to have regular morphology, suggesting the success growth of purely inclined nanowires on the GaAs $\{\bar{1}\bar{1}\bar{1}\}$ substrate.

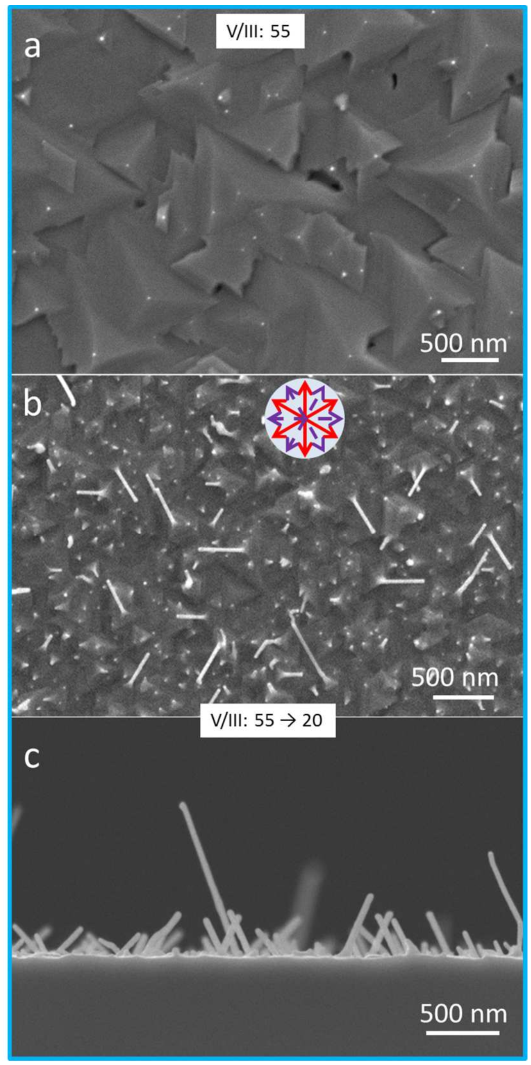

Fig. 3 (a) Tilt SEM image of InAs growth at a single-V/III-ratio of ~55. (b, c) SEM images of InAs nanowires grown by the two-V/III-ratio procedure (first at a V/III ratio of ~55, and switch to a V/III ratio of ~20). (b) Top-view SEM image. The inset showing a sketch of the orientation relationship between <112> (purple) and <110> (red) directions. (c) Side-view SEM image.

TEM investigations were performed on these inclined nanowires to determine their structural characteristics. Fig. 4a shows the overview of a typical inclined nanowire. In strong contrast to the short inclined nanowires found in the previous sample (refer to Fig. 1 and 2), the inclined nanowires in this sample have perfect morphology. Fig. 4b is low-magnified HRTEM image showing no lattice defects in a larger area and Fig. 4c is a <110> zone-axis HRTEM image, in which the nanowire is shown to have the zinc-blende structure as expected. The inset in Fig. 4c is the corresponding fast Fourier transform (FFT). From which, the <110> growth direction of the nanowire can be clarified. Our extensive HRTEM studies on over a dozen of inclined nanowires confirmed this defect-free zinc-blende structure nature along entire nanowires and they are indeed grown along the <110> directions. In this regard, the growth of pure defect-free zinc-blende structured nanowires has been successfully achieved by our two-V/III-ratio procedure in MBE. It should be noted that the growth directions of our inclined nanowires is different to those inclined nanowires induced by the multiple-order twinning.[36, 37] In their cases, multiple-order twinning induced non-vertical nanowires still belong to one of the <111> directions, however, our inclined nanowires belong to the non-<111> directions. It has been documented that the growth directions of nanowires can affect their properties,[38, 39] so that our defect-free nanowires grown in the non-<111> directions would have different properties when compared with those conventional <111> nanowires.

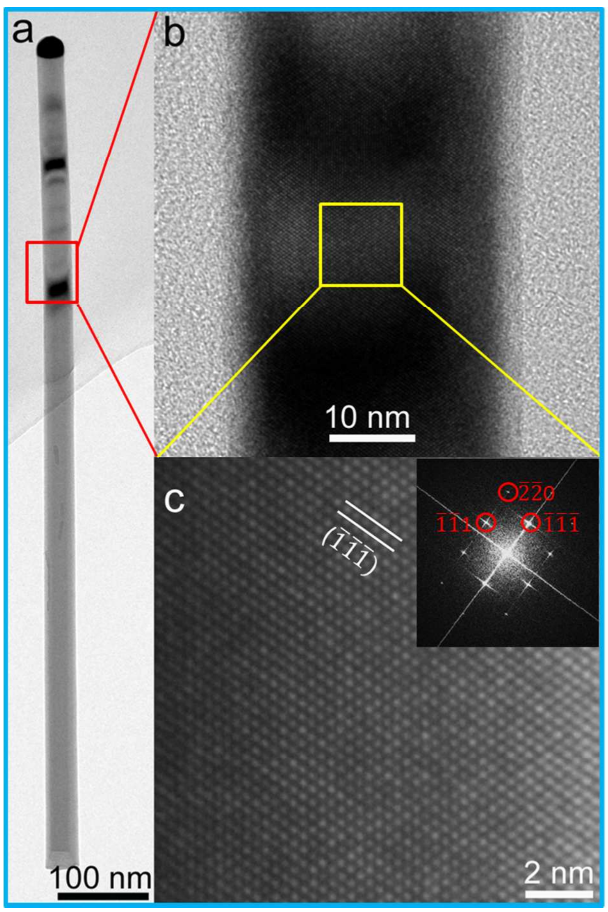

Fig. 4 TEM investigations of InAs nanowires from newly designed growth. (a) The overview of a typical nanowire. (b) Low-magnified HRTEM image taken from the top of nanowire as marked in (a). (c) <110> zone-axis HRTEM image taken from the marked area in (b), and the inset is the corresponding FFT.

Based on these experimental results and discussion outlined above, different growth models of Au-catalyzed InAs nanowires on the GaAs {$\bar{1}\bar{1}\bar{1}$} substrates in MBE can be summarized, as schematically illustrated in Fig. 5. After the annealing process, catalyst droplets were formed on the GaAs substrate, as shown in Fig. 5a. When the growth was conducted by a single V/III ratio procedure with a high V/III ratio (~45), only the vertical nanowires and triangular pyramids can be induced, as illustrated in Fig. 5b, and experimentally confirmed in Fig. 5c. With a nanowire growth under a lower single V/III ratio (~20), both vertical and inclined nanowires can be induced simultaneously, as illustrated in Fig. 5d and experimentally demonstrated in Fig. 5e.[35] The formation of our inclined nanowires under a low V/III ratio can be explained by the well-proved nanowire nucleation model[28, 31], which suggested that the nucleation energy barrier for the growth of inclined nanowires is higher than that of vertical nanowires. Therefore, the inclined nanowires can be induced at a relatively low V/III ratio and/or at a higher catalyst supersaturation which would decrease the nucleation energy barrier. Importantly, if the nanowire growth was carried out under a two-V/III-ratio procedure with a high-V/III ratio of ~55 first followed by a low-V/III ratio of ~20, defect-free and zinc-blende structured nanowires can be induced. As illustrated in Fig. 5f , with the growth of a high V/III ratio (~55), only the triangular pyramids were formed during InAs growth, and when the V/III ratio is consequently lowered (to ~20), defect-free and zinc-blende structured nanowires can be grown from these pyramids, as shown schematically in Fig. 5f and experimentally in Fig. 5h. Therefore, as can be witnessed in SEM images shown in Fig. 5c, 5e and 5h, by manipulating the V/III ratio and performing a two-V/III-ratio procedure, controlled growths of solely vertical wurtzite structured InAs nanowires, the mixture of vertical and inclined nanowires, and solely inclined defect-free zinc-blende structured nanowires can be realized.

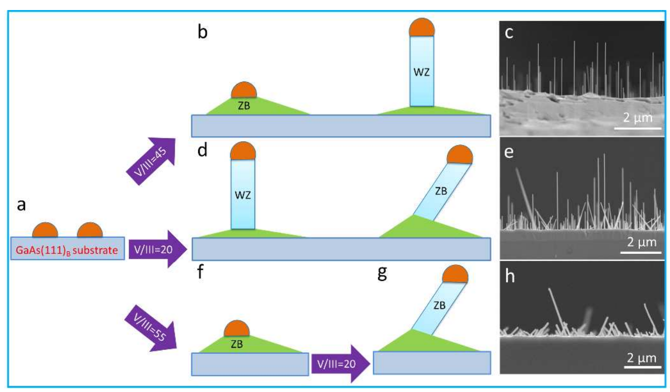

Fig. 5 Schematic illustrating the controlled growth of InAs nanowires under different V/III ratios and different growth procedures.

Conclusions

In conclusion, we demonstrated the controlled growth of high-quality zinc-blende structured InAs nanowires in MBE by a two-V/III-ratio procedure which consists of a high-V/III ratio growth step to prepare the nanowire foundation on the substrate surface, followed by a low-V/III ratio step to induce nanowire growth. By tuning the V/III ratios in the two-V/III-ratio procedure, we have successfully achieved the growth of pure defect-free zinc-blende structured InAs nanowires in MBE. This novel growth approach provides a new strategy to control the crystal structure and quality of semiconductor nanowires.

Acknowledgements

This study is financially supported by the Australian Research Council, the National Basic Research Program of China, and the National Science Foundation of China. Australian Microscopy & Microanalysis Research Facility is also gratefully acknowledged for providing microscopy facilities for this study.

Notes and references

[a] Materials Engineering, The University of Queensland, St. Lucia, QLD 4072, Australia
[b] National Laboratory for Infrared Physics, Shanghai Institute of Technical Physics, Chinese Academy of Sciences, 500 Yu-Tian Road, Shanghai 200083, China
[c] Centre for Microscopy and Microanalysis, The University of Queensland, St. Lucia, QLD 4072, Australia

1 X. F. Duan, Y. Huang, Y. Cui, J. F. Wang and C. M. Lieber, *Nature*, 2001, **409**, 66.
2 H. Xia, Z. Y. Lu, T. X. Li, P. Parkinson, Z. M. Liao, F. H. Liu, W. Lu, W. D. Hu, P. P. Chen, H. Y. Xu, J. Zou and C. Jagadish, *ACS Nano*, 2012, **6**, 6005.
3 N. Guo, W. D. Hu, L. Liao, S. Yip, J. C. Ho, J. D. Miao, Z. Zhang, J. Zou, T. Jiang, S. J. Wu, X. S. Chen and W. Lu, *Adv. Mater.*, 2014, **26**, 8232.
4 P. Krogstrup, H. I. Jorgensen, M. Heiss, O. Demichel, J. V. Holm, M. Aagesen, J. Nygard and A. Fontcuberta i Morral, *Nature Photonics*, 2013, **7**, 306.
5 Y. N. Guo, H. Y. Xu, G. Auchterlonie, T. Burgess, H. J. Joyce, Q. Gao, H. H. Tan, C. Jagadish, H. B. Shu, X. S. Chen, W. Lu, Y. Kim and J. Zou, *Nano Lett.*, 2013, **13**, 643.
6 J. Zou, M. Paladugu, H. Wang, G. J. Auchterlonie, Y. N. Guo, Y. Kim, Q. Gao, H. J. Joyce, H. H. Tan and C. Jagadish, *Small*, 2007, **3**, 389.
7 H. Y. Xu, Y. Wang, Y. N. Guo, Z. M. Liao, Q. Gao, N. Jiang, H. H. Tan, C. Jagadish and J. Zou, *Cryst. Growth Des.*, 2012, **12**, 2018.
8 Z. Zhang, Z. Y. Lu, P. P. Chen, H. Y. Xu, Y. N. Guo, Z. M. Liao, S. X. Shi, W. Lu and J. Zou, *Appl. Phys. Lett.*, 2013, **103**, 073109.
9 V. G. Dubrovskii, *Appl. Phys. Lett.*, 2014, **104**, 053110.
10 T. Rieger, M. Luysberg, T. Schaepers, D. Gruetzmacher and M. I. Lepsa, *Nano Lett.*, 2012, **12**, 5559.
11 L. E. Jensen, M. T. Bjork, S. Jeppesen, A. I. Persson, B. J. Ohlsson and L. Samuelson, *Nano Lett.*, 2004, **4**, 1961.
12 R. S. Wagner and W. C. Ellis, *Appl. Phys. Lett.*, 1964, **4**, 89.
13 A. I. Persson, M. W. Larsson, S. Stenstrom, B. J. Ohlsson, L. Samuelson and L. R. Wallenberg, *Nat. Mater.*, 2004, **3**, 677.
14 P. Caroff, K. A. Dick, J. Johansson, M. E. Messing, K. Deppert and L. Samuelson, *Nature Nanotechnology*, 2009, **4**, 50.
15 F. Glas, J.-C. Harmand and G. Patriarche, *Phys. Rev. Lett.*, 2007, **99**, 146101.
16 S. Shi, Z. Zhang, Z. Lu, H. Shu, P. Chen, N. Li, J. Zou and W. Lu, *Nanoscale Res. Lett.*, 2015, **10**, 108.
17 H. A. Fonseka, P. Caroff, J. Wong-Leung, A. S. Ameruddin, H. H. Tan and C. Jagadish, *Acs Nano*, 2014, **8**, 6945.
18 J. Johansson, J. Bolinsson, M. Ek, P. Caroff and K. A. Dick, *Acs Nano*, 2012, **6**, 6142.
19 R. E. Algra, M. A. Verheijen, L.-F. Feiner, G. G. W. Immink, W. J. P. van Enckevort, E. Vlieg and E. P. A. M. Bakkers, *Nano Lett.*, 2011, **11**, 1259.
20 S. Lehmann, J. Wallentin, D. Jacobsson, K. Deppert and K. A. Dick, *Nano Lett.*, 2013, **13**, 4099.
21 K. Ikejiri, Y. Kitauchi, K. Tomioka, J. Motohisa and T. Fukui, *Nano Lett.*, 2011, **11**, 4314.
22 A. S. Ameruddin, H. A. Fonseka, P. Caroff, J. Wong-Leung, R. L. O. h. Veld, J. L. Boland, M. B. Johnston, H. H. Tan and C. Jagadish, *Nanotechnology*, 2015, **26**, 205604.
23 H. J. Joyce, Q. Gao, H. H. Tan, C. Jagadish, Y. Kim, X. Zhang, Y. N. Guo and J. Zou, *Nano Lett.*, 2007, **7**, 921.
24 J. J. Hou, N. Han, F. Wang, F. Xiu, S. Yip, A. T. Hui, T. Hung and J. C. Ho, *Acs Nano*, 2012, **6**, 3624.
25 Q. D. Zhuang, E. A. Anyebe, R. Chen, H. Liu, A. M. Sanchez, M. K. Rajpalke, T. D. Veal, Z. M. Wang, Y. Z. Huang and H. D. Sun, *Nano Lett.*, 2015, **15**, 1109.
26 H. Y. Xu, Y. Wang, Y. N. Guo, Z. M. Liao, Q. Gao, H. H. Tan, C. Jagadish and J. Zou, *Nano Lett.*, 2012, **12**, 5744.
27 U. Krishnamachari, M. Borgstrom, B. J. Ohlsson, N. Panev, L. Samuelson, W. Seifert, M. W. Larsson and L. R. Wallenberg, *Appl. Phys. Lett.*, 2004, **85**, 2077.
28 J. Wang, S. R. Plissard, M. A. Verheijen, L.-F. Feiner, A. Cavalli and E. P. A. M. Bakkers, *Nano Lett.*, 2013, **13**, 3802.
29 H. Shtrikman, R. Popovitz-Biro, A. Kretinin and M. Heiblumf, *Nano Lett.*, 2009, **9**, 215.
30 Z. Zhang, K. Zheng, Z. Y. Lu, P. P. Chen, W. Lu and J. Zou, *Nano Lett.*, 2015, **15**, 876.
31 Z. Zhang, Z. Y. Lu, H. Y. Xu, P. P. Chen, W. Lu and J. Zou, *Nano Res.*, 2014, **7**, 1640.
32 Z. M. Liao, Z. G. Chen, Z. Y. Lu, H. Y. Xu, Y. N. Guo, W. Sun, Z. Zhang, L. Yang, P. P. Chen, W. Lu and J. Zou, *Appl. Phys. Lett.*, 2013, **102**, 063106.
33 D. L. Dheeraj, G. Patriarche, H. Zhou, T. B. Hoang, A. F. Moses, S. Gronsberg, A. T. J. van Helvoort, B.-O. Fimland and H. Weman, *Nano Lett.*, 2008, **8**, 4459.
34 F. Martelli, S. Rubini, F. Jabeen, L. Felisari and V. Grillo, *J. Cryst. Growth*, 2011, **323**, 297.
35 Z. Zhang, Z. Lu, P. Chen, W. Lu and J. Zou, *Acta Mater.*, 2015, **92**, 25.
36 E. Uccelli, J. Arbiol, C. Magen, P. Krogstrup, E. Russo-Averchi, M. Heiss, G. Mugny, F. Morier-Genoud, J. Nygard, J. Ramon Morante and A. Fontcuberta i Morral, *Nano Lett.*, 2011, **11**, 3827.
37 E. Russo-Averchi, M. Heiss, L. Michelet, P. Krogstrup, J. Nygard, C. Magen, J. R. Morante, E. Uccelli, J. Arbiol and A. Fontcuberta i Morral, *Nanoscale*, 2012, **4**, 1486.

38 A. H. Chin, T. S. Ahn, H. Li, S. Vaddiraju, C. J. Bardeen, C.-Z. Ning and M. K. Sunkara, *Nano Lett.*, 2007, **7**, 626.
39 J. Bao, D. C. Bell, F. Capasso, J. B. Wagner, T. Martensson, J. Tragardh and L. Samuelson, *Nano Lett.*, 2008, **8**, 836.

Table of Content

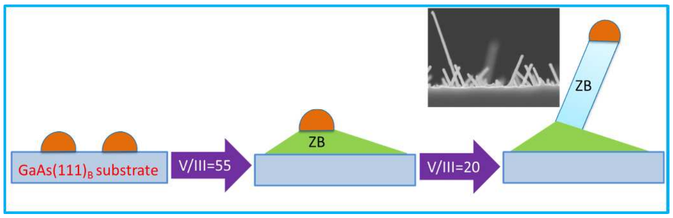

A two-V/III-ratio process to control the growth of pure defect-free zinc-blende structured InAs nanowires.